

The magnetospheric activity of bare strange quark stars

Junwei Yu and Renxin Xu

*School of Physics and State Key Laboratory of Nuclear Physics and Technology,
Peking University, Beijing 100871, China*

J.W.Yu@pku.edu.cn; r.x.xu@pku.edu.cn

ABSTRACT

The normal neutron star model of pulsar-like stars suffers a severe problem, the binding energy problem that both ions (e.g., $^{56}_{26}\text{Fe}$) and electrons on normal neutron star surface can be pulled out freely by the monopole-induced electric field so that sparking on polar cap can hardly occur. In this paper, we extensively study this problem in a bare strange quark star (BSS) model. We find that the huge potential barrier established by the electric field in the vacuum gap above polar cap could usually prevent electrons from flowing out unless the electric potential of a pulsar is sufficiently lower than that at infinite interstellar medium. Other processes, such as the diffusion of electrons, thermionic emission and tunneling effect of electrons penetrating the potential barrier have also been included here. We demonstrate that both positive and negative particles on a BSS's surface would be bound strongly enough to form a vacuum gap above its polar cap as long as the BSS is not charged (or not highly negative charged), and multi-accelerators could occur in a BSS's magnetosphere. Our results would be helpful to distinguish normal neutron stars and bare quark stars through pulsar's magnetospheric activities.

Subject headings: elementary particles — pulsars: general — pulsars: stars — neutron

1. Introduction

Although pulsar-like stars have many different manifestations, they are populated mainly by rotation-powered radio pulsars. A lot of information about pulsar radiative process is inferred from the integrated and individual pulses, the sub-pulses, and even the micro-structures of radio pulses. Among the magnetospheric emission models, the user-friendly

nature of Ruderman & Sutherland (1975; hereafter RS75) model is a virtue not shared by others (Shukre 1992).

In RS75 and its modified versions (e.g., Qiao & Lin 1998), a vacuum gap exists above polar cap of a pulsar, in which charged particles (electrons and positrons) are accelerated because of $\mathbf{E} \cdot \mathbf{B} \neq 0$. These accelerated charged particles, moving along the curved magnetic field lines, radiate curvature or ICS-induced high energy photons which are again converted to e^\pm in strong magnetic field. A follow-up breakdown of the vacuum gap produces secondary pair plasma that radiate coherent radio emission. These models with gap-sparking provide a good framework to analyze observational phenomena, especially the drifting (Drake & Craft 1968; Deshpande & Rankin 1999; Vivekanand & Joshi 1999) and bi-drifting (Qiao et al. 2004) sub-pulses.

However, the RS75-like vacuum gap models work only in strict conditions: strong magnetic field and low temperature on surface of pulsars with $\boldsymbol{\Omega} \cdot \mathbf{B} < 0$ (e.g., Gil et al. 2006; Medin & Lai 2007), where $\boldsymbol{\Omega}$ is the angular frequency and \mathbf{B} is the magnetic field. The necessary binding energy of positive ions (e.g., $^{56}_{26}\text{Fe}$) for RS75 model to work should be higher than ~ 10 keV, while calculations showed that the cohesive energy of $^{56}_{26}\text{Fe}$ at the neutron star surface is < 1 keV (Fowlers et al. 1977; Lai 2001). This binding energy problem could be solved within a partially screened inner gap model (Gil et al. 2006; Melikidze & Gil 2009) for normal neutron stars with $\boldsymbol{\Omega} \cdot \mathbf{B} < 0$. Alternatively, it is noted that the binding energy could be sufficiently high for any $\boldsymbol{\Omega} \cdot \mathbf{B}$ if pulsars are bare strange quark stars (Xu & Qiao 1998; Xu et al. 1999, 2001) although strange stars were previously supposed to exist with crusts (Alcock et al. 1986). Certainly, it is very meaningful in the elementary strong interaction between quarks and the phases of cold quark matter that the binding energy problem be solved by bare quark stars as pulsars (Xu 2009).

Though the ideas of solving the binding energy problem in BSS model were presented and discussed in some literatures, there is no comprehensive study with quantitative calculations up-to-date. In this paper, we are going to investigate the BSS model in quantitative details and show the binding of particles on BSS's surface with clear physical pictures. Our research result is that multi-accelerators could occur above a polar cap, and for most cases, particles on a BSS's surface are bound strongly enough to form a vacuum gap above the polar cap and RS75-like models work well if pulsars are BSSs.

2. The accelerators above polar caps of BSSs

On a BSS's surface, there are positively (u -quarks) and negatively (d - and s -quarks and electrons) charged particles. Quarks are confined by strong color interaction, whose binding energy could be considered as infinite when compared to the electric force, while electrons are bound by electro-magnetic interaction. Therefore, in this paper we focus on the binding of electrons.

2.1. The energy of electrons on Fermi surface

The distribution of electrons in BSSs is described in the Thomas-Fermi model (Alcock et al. 1986). In this model, equilibrium of electrons in an external electric field assures that the total energy of each electron on Fermi surface is a constant. For the case of extremely relativistic degenerate electron gas, it gives (Alcock et al. 1986)

$$\epsilon(r) = cp_F - e\varphi(r) = \phi_0, \quad (1)$$

where $\epsilon(r)$ is the total energy, cp_F is the Fermi energy, $-e\varphi(r)$ is the electrostatic potential energy of electrons and ϕ_0 is a constant.

On the other hand, the potential distribution of electrons on the star's surface due to the electric field induced by the rotating, uniformly magnetized star, for the sake of simplicity, could be assumed and estimated as (Xu et al. 2006, Eq. 2 there)

$$V_i(\theta) \simeq 3 \times 10^{16} B_{12} R_6^2 P^{-1} \sin^2 \theta \text{ (V)} + V_0, \quad (2)$$

where $B_{12} = B/(10^{12} \text{ G})$, $R_6 = R/(10^6 \text{ cm})$ is the radius of a pulsar, $P = 2\pi/\Omega$ is the pulsar period, θ is the polar angle and V_0 is another constant. The potential energy related to Eq. (2), eV_i , could be regarded as the constant, ϕ_0 , in Eq. (1). The choice of zero potential for electrons is very important. Two scenarios could be possible here. The first scenario is that we choose the critical field lines whose feet are at the same electric potential as the interstellar medium (Goldreich & Julian 1969) as the zero potential. We may also suggest a second choice that the zero potential should be at those magnetic field lines which separate annular and core regions determined by $S_{AG} = S_{CG}$, where S_{AG} and S_{CG} , are the stellar surface areas of annular region and core region, respectively. The second scenario is based on the idea that if particles with opposite charge flow out with ρ_{GJ} in both regions, the area of this two regions should approximately be equal in order to keep the star not charging. The feet of the critical field lines and the magnetic field lines determined by $S_{AG} = S_{CG}$ are designated as C and B, respectively (Fig. 1). For the above two scenarios, the potential

energy, $\phi_i = eV_i$, of electrons at the surface from the pole to the equator plane are given by

$$\phi_{i,C}(\theta) \simeq -3 \times 10^{10} B_{12} R_6^2 P^{-1} (\sin^2 \theta - \sin^2 \theta_C) \text{ MeV}, \quad (3)$$

and

$$\phi_{i,B}(\theta) \simeq -3 \times 10^{10} B_{12} R_6^2 P^{-1} (\sin^2 \theta - \sin^2 \theta_B) \text{ MeV}, \quad (4)$$

respectively, where θ_C and θ_B are polar angles of C and B. This potential energy of electrons is higher at the poles and decreases toward the equator for an ‘antipulsar’ of $\mathbf{\Omega} \cdot \mathbf{B} > 0$, which means that electrons in different regions above a polar cap may behave differently.

2.2. The potential barrier of electrons in vacuum gap

The behavior of electrons is determined by their potential distribution on polar caps of pulsars, i.e., the potential energy distribution in vacuum gap and the stellar surface. Unlike RS75, we consider the situation of an ‘antipulsar’ with the magnetic axis parallel to the spin axis. A schematic representation for ‘antipulsar’ is showed in figure 1. Following RS75, the zero potential surface should be on the top of the vacuum gap at which the gap electric field vanishes. Thus the potential energy distribution of electrons in vacuum gap, in one-dimensional approximation, is (RS75)

$$\phi_p(Z) = 2\pi \times 10^4 P^{-1} B_{12} (h_3 - Z_3)^2 \text{ MeV}, \quad (5)$$

where $h_3 = h/(10^3 \text{ cm})$ is the height of vacuum gap, $Z_3 = Z/(10^3 \text{ cm})$ is the space coordinate measuring height above the quark surface. This potential energy distribution established a huge potential barrier for electrons, which may prevent electrons escaping into pulsar’s magnetosphere. The height of this potential barrier mainly depends on the height of vacuum gap which is determined by cascade mechanics of sparking, i.e., the curvature-radiation-induced (CR-induced) cascade sparking and the resonant inverse-Compton-scattering-induced (ICS-induced) cascade sparking. In CR-induced cascade sparking model, the gap height is (RS75)

$$h_{\text{CR}} = 5 \times 10^3 \rho_6^{2/7} B_{12}^{-4/7} P^{3/7} \text{ cm}, \quad (6)$$

and in ICS-induced cascade sparking model, it is (Zhang et al. 2000)

$$h_{\text{ICS}} = 2.79 \times 10^4 \rho_6^{4/7} B_{12}^{-11/7} P^{1/7} \text{ cm}. \quad (7)$$

The potential energy distribution for electrons in the gap for CR-induced cascade sparking model of typical normal pulsars (NPs) is plotted in figure 2, in which the potential energy of electrons at the stellar surface, namely ϕ_i , is illustrated at different polar angles. The

Fig. 1.— A schematic representation of the geometry of ‘antipulsars’. CFL stands for the critical field lines, NCS for null charge surface, and LC for light cylinder. The enlarged arrows with opposite directions in annular region and core region represent the directions of the electric field in vacuum gap. "A", "B" and "C" represent the feet of different magnetic field lines (see text).

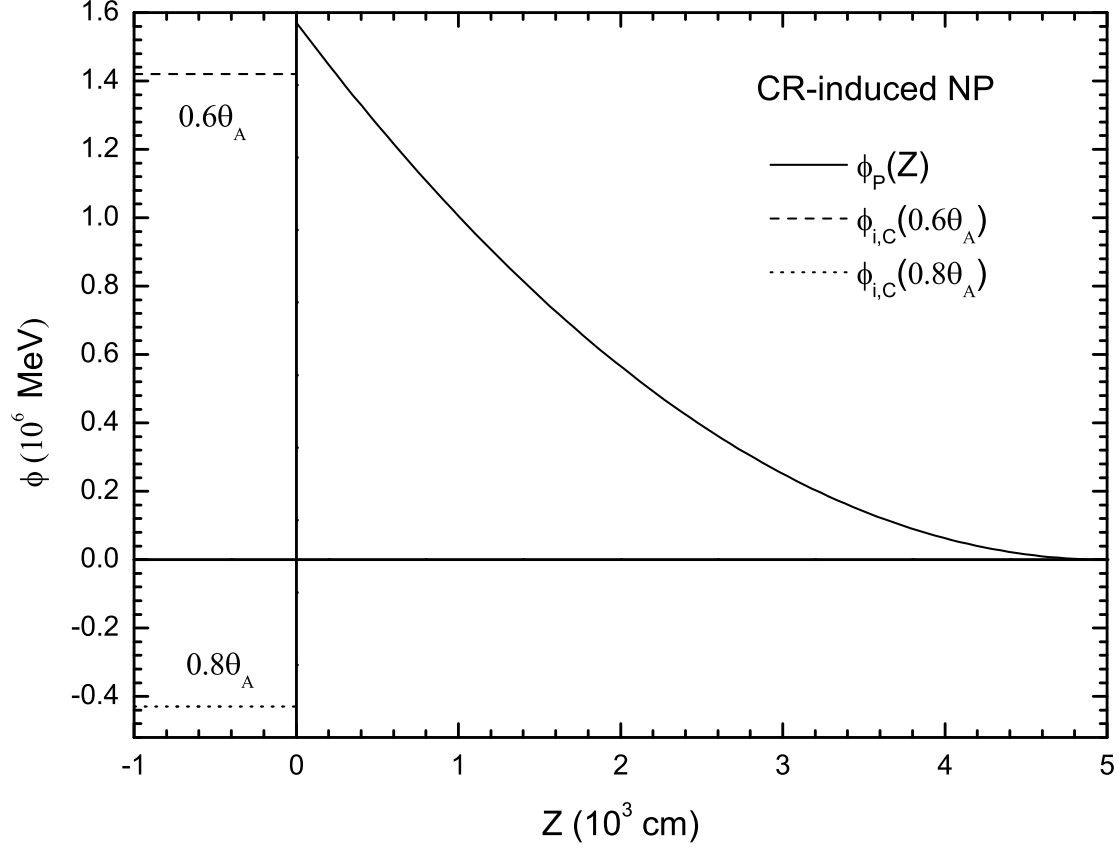


Fig. 2.— The potential energy distributions for typical NPs ($P = 1$ s, $B = 10^{12}$ G). The potential energy of electrons at stellar surface, namely $\phi_i(\theta)$, is illustrated with fixed polar angles, for example, with $0.6\theta_A$ and $0.8\theta_A$, where θ_A is the polar angle of the feet of the last open field lines (Fig. 1), and ϕ_P is the potential energy distribution of electrons in vacuum gap.

situation of CR-induced cascade sparking of typical millisecond pulsars (MSPs) is similar to that of NPs but with greater height of potential barrier.

Comparing the potential barrier with energy of electrons on Fermi surface, we will obtain clearly physical picture of electrons above polar cap. Namely, only electrons with energy greater than the potential barrier can escape into pulsar’s magnetosphere. It is known that energy of electrons is a function of polar angle (Eq. 3 and 4). As a result, there may be a critical polar angle, θ_0 , at which the energy of electrons equals to the height of this potential barrier. Compare between energy of electrons and the height of potential barrier on stellar surface for typical NPs of CR-induced sparking is showed in figure 3 (θ_0 does not exist for both ICS-induced sparking of NPs and MSPs, see table 1). The results are as follow: free flow status stays in the region of $[0, \theta_0]$ and vacuum gap in $[\theta_0, \theta_A]$ for ‘antipulsars’, where θ_A is polar angle of the feet of the last open field lines (Fig. 1). We give the results of θ_0 in table 1 and find that in the case of CR-induced sparking NPs, free flow and vacuum gap coexist above polar cap which differs from the previous scenario. The general case is that only vacuum gap exists.

2.3. The effects of thermionic emission and diffusion of electrons

Now we know that electrons inside BSSs usually cannot escape into magnetospheres. Does any other process which will affect the existence of vacuum gap above polar cap? In vacuum gap, except pulling electrons from the interior of BSSs, two other processes which may also prevent vacuum gap from being formed require to be investigated. One is the thermionic emission of electrons and another is the diffusion of electrons from the outer edge to the inner region of polar cap. For the first one, if the current density due to thermionic emission of electrons is much smaller than that of Goldreich-Julian charge density, the vacuum gap survives as well. This current density is determined by the Richard-Dushman equation (Usov & Melrose 1995)

$$J_{\text{th}} = \frac{em_e}{2\pi\hbar^3} \times (k_B T)^2 \exp\left(-\frac{\phi}{k_B T}\right) = 1.2 \times 10^{14} T_6^2 \exp(-1.161 \times 10^4 T_6^{-1} \phi_{\text{MeV}}) \text{ A cm}^{-2}, \quad (8)$$

where m_e is the mass of electron, k_B is the Boltzmann constant, $T_6 = T/(10^6 \text{ K})$ is the temperature and $\phi_{\text{MeV}} = \phi/\text{MeV}$ is the work function of electrons. In the vacuum gap of BSSs, the work function of thermionic electrons is the order of the difference between the height of the potential barrier and the potential energy of electron at the surface of BSSs. The order of the difference is about 10^6 MeV . At the same time, the temperature of BSSs is about 10^6 K . Thus, the thermionic emission current density is ~ 0 , which means that the thermionic emission of electrons can not affect the existence of the vacuum gap.

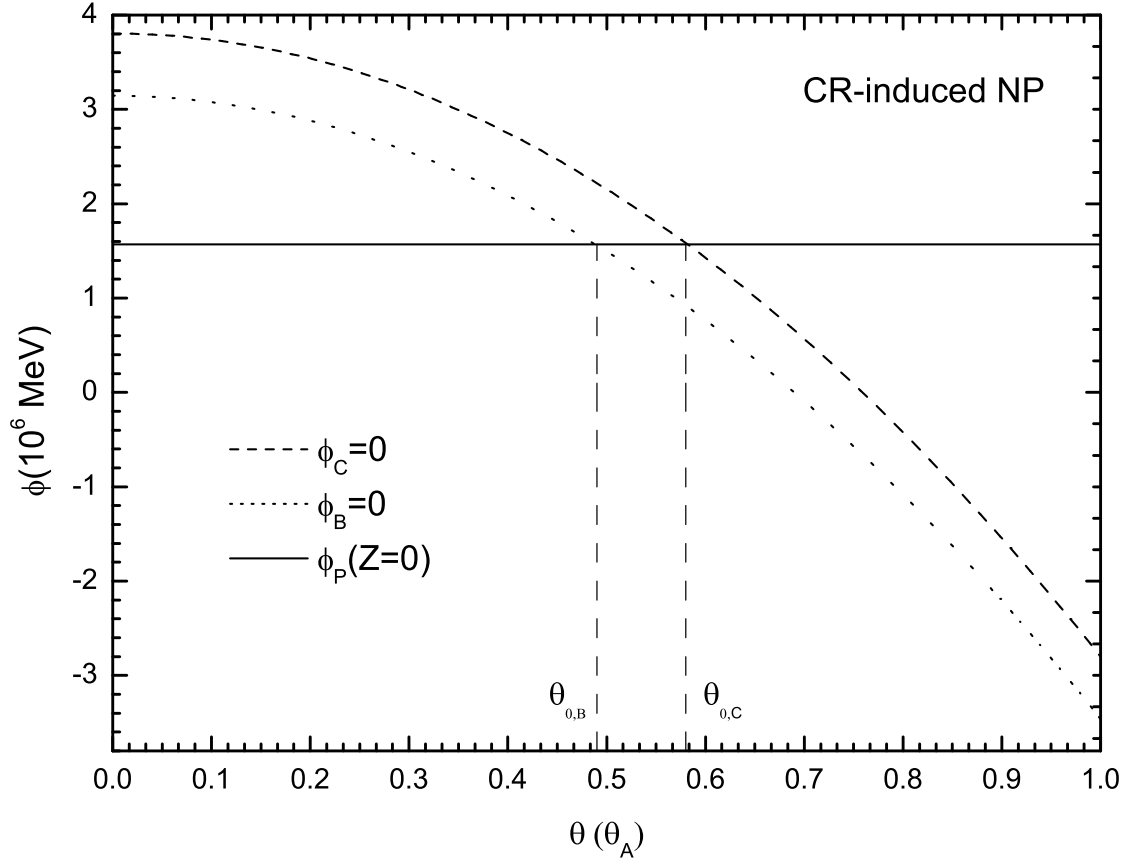


Fig. 3.— The potential energy distribution on stellar surface of typical NPs with the choice of $\phi_i(\theta_C) = 0$ and $\phi_i(\theta_B) = 0$, respectively. The solid horizontal line is the potential energy of electrons in the gap electric field at the stellar surface, namely $\phi_P(Z = 0)$.

The second process is the diffusion of electrons whose distribution above BSSs surface is (Xu et al. 2001)

$$n_e(Z) = \frac{1.187 \times 10^{32} \phi_{q,\text{MeV}}^3}{(0.06 \phi_{q,\text{MeV}} Z_{11} + 4)^3} \text{ cm}^{-3}. \quad (9)$$

The number density (so does the kinetic energy density, ϵ_k) decreases rapidly with the increasing of the distance from quark matter surface at which $\epsilon_k \gg \epsilon_B$, where ϵ_B , is the magnetic field energy density. As a result, there is a balance surface where the kinetic energy density equals to the magnetic energy density. Below this balance surface, electrons can cross magnetic field lines freely and above the balance surface, this motion is prevented. Making use of $\epsilon_k = \epsilon_B$, where $\epsilon_k = n_e \epsilon_F$ (ϵ_F is the Fermi energy of degenerate electrons) and $\epsilon_B = B^2/8\pi$, we can obtain the height of the balance surface. For NPs, it is $Z_{11} \simeq 160 \ll Z_{0,11} \simeq 7000$ at which the gap electric field begins to dominate, and for MSPs, it is $Z_{11} \simeq 1.7 \times 10^4 \ll Z_{0,11} \simeq 6.3 \times 10^6$, where $Z_{11} = Z/(10^{-11} \text{ cm})$. The diffusion of electrons beneath $Z_{0,11}$ is still confined by the surface electric field meaning that only the diffusion of electrons above the surface with height of Z_0 needs to be considered. The diffusion coefficient, D_c , is given by (Xu et al. 2001)

$$D_c \simeq \frac{\rho^2}{\tau_F} = \frac{\pi n_e c e^2}{B^2} = 2.17 \times 10^{-3} B_{12}^{-2} n_{e,29} \text{ cm}^2 \text{ s}^{-1}, \quad (10)$$

where $\rho = \gamma \rho_L$ ($\rho_L = m_e v c / (eB)$ is the Larmor radius) is the cyclotron radius of relativistic electrons, and $\tau_F \simeq \gamma m_e^2 v^3 / (\pi e^4 n_e)$ is the mean free flight time of electrons. The gradient of electrons along with the diffusion direction is approximately

$$\frac{dn_e}{dx} \simeq \frac{n_e}{\rho} = 1.4 \times 10^{38} n_{e,29}^{2/3} \text{ cm}^{-4}. \quad (11)$$

Thus, the diffusion rate is

$$I_{\text{df}} = 2.77 \times 10^{29} B_{12}^{-1} P^{-1/2} R_6^{3/2} \int_{Z_{0,11}}^{\infty} n_{e,29}^{5/3} dZ_{11} \text{ s}^{-1}, \quad (12)$$

where $n_{e,29} = n_e / (10^{29} \text{ cm}^{-3})$. For NPs, we have $I_{\text{df}} \simeq 4.75 \times 10^{24} \text{ s}^{-1}$, $4.91 \times 10^{24} \text{ s}^{-1}$ and $4.93 \times 10^{24} \text{ s}^{-1}$ for $\phi_q = 1, 10$ and 20 MeV , respectively. For MSPs, $I_{\text{df}} \simeq 7.52 \times 10^{17} \text{ s}^{-1}$, $7.52 \times 10^{17} \text{ s}^{-1}$ and $7.53 \times 10^{17} \text{ s}^{-1}$ for $\phi_q = 1, 10$ and 20 MeV , respectively. On the other hand, the flow with the Goldreich-Julian flux is $I_{\text{GJ}} = \pi r_p^2 n_{\text{GJ}} c \simeq 1.4 \times 10^{30} P^{-2} R_6^3 B_{12} \text{ s}^{-1}$. Both have $I_{\text{df}} \ll I_{\text{GJ}}$ for NPs and MSPs. That means that the diffusion of electrons is also negligible which guarantees the existence of vacuum gap.

3. Conclusions and Discussions

The binding energy problem is one of the most serious problems in neutron star model of pulsar-like stars. Arons and Scharlemann (1979) developed an alternative model, the space-charge limited flow (SCLF) model, in which the particles, both iron ions and electrons can be pulled out freely, and form a steady flow (Aron & Scharlemann 1979). In this SCLF model, the drifting subpulse phenomenon which has been observed in many pulsars, including PSR B0943+10, can rarely be reproduced. The prerequisite for understanding this phenomenon could be the existence of a vacuum gap.

In our calculations, we found that there is a new physical scenario for CR-induced sparking of NPs that free flow and vacuum gap may coexist above the polar cap. But in other cases, such as ICS-induced sparking of NPs and MSPs, only vacuum gap exists. In general, if a pulsar is not highly negatively charged (Xu et al. 2006), vacuum gap survives at polar cap as well. One limitation of our model is that our calculation is based on one-dimensional approximation and it might fail in some cases of MSPs. As far as we find, it is very difficult to deal with the high-dimensional cases. The one-dimensional approximation provides a good understanding of the geometry of polar cap of BSSs. Here are the mainly results we obtained. The binding energy problem could be solved completely in the BSS model of pulsar as long as BSSs are neutral (or not highly negative charged). The structure of polar cap of BSSs are very different with respect to that of NSs. Detailed information about the geometry of BSS's polar cap is given in table 2.

A more interesting region from pole to equator may locate at $[\theta_0, \theta_C]$ or $[\theta_0, \theta_B]$ of CR-induced sparking NPs. After the birth of a NP, a vacuum gap exists at this region. Once sparking starts, the potential energy drops rapidly due to screen of pairs which will become lower than that of the monopole-induced, namely $V_i(\theta)$ at the surface. As a result, the sparking converts vacuum gap to free flow at this region until the sparking ends, i.e., at $[\theta_0, \theta_C]$ or $[\theta_0, \theta_B]$, vacuum gap and free flow exist alternately. This argument may have profound implications for us to distinguish neutron stars and quark stars by pulsar's magnetospheric activities (e.g., the diversity pulse profiles).

We assume the potential energy related to Eq. (2), eV_i , to be the constant, ϕ_0 , in Eq. (1). This assumption could be reasonable. For an uniformly magnetized, rotating conductor sphere, the homopolar generator will induce an electric field which is a function of polar angle, as described in Eq. (2). In the case of $\mathbf{\Omega} \cdot \mathbf{B} > 0$ (Fig. 1), the potential energy of electron is highest at the polar region which means that those electrons there could be easier to escape. An alternative picture below results qualitatively the same conclusion. Because of Lorentz force inside a star, more electrons locate at the polar region so that the Fermi energy of electron is higher there and easier to escape into magnetosphere.

Table 1. The polar angles of θ_B , θ_C and θ_0 for both CR-induced and ICS-induced sparking of typical NPs and MSPs within both the choice of zero potentials.

			$\theta_{0,B} (\theta_A)$		$\theta_{0,C} (\theta_A)$			
	θ_A (rad)	$\theta_B (\theta_A)$	$\theta_C (\theta_A)$	CR	ICS	CR	ICS	
NPs	0.0145	0.69	0.76	0.49	...	0.58	...	$\Omega \cdot \mathbf{B} > \mathbf{0}^b$
				0.84	2.76 ^a	0.90	2.83 ^a	$\Omega \cdot \mathbf{B} < \mathbf{0}^c$
				$\Omega \cdot \mathbf{B} > \mathbf{0}$
MSPs	0.145	0.69	0.76	1.49 ^a	...	1.52 ^a	...	$\Omega \cdot \mathbf{B} < \mathbf{0}$

^a $\theta_0 > \theta_A$, which means that the whole polar cap region is vacuum gap.

^bantipulsar.

^cpulsar.

Table 2. The accelerators above polar caps of BSSs

		$[0, \theta_0]^\dagger$		$[\theta_0, \theta_A]$		
		CR	ICS	CR	ICS	
NPs	SCLF	VG	VG	VG	VG	$\Omega \cdot \mathbf{B} > \mathbf{0}$
	VG	VG [‡]	SCLF	VG [‡]	VG [‡]	$\Omega \cdot \mathbf{B} < \mathbf{0}$
	VG	VG	VG	VG	VG	$\Omega \cdot \mathbf{B} > \mathbf{0}$
MSPs	VG [‡]	VG	VG [‡]	VG	VG	$\Omega \cdot \mathbf{B} < \mathbf{0}$

[†] θ_0 represents $\theta_{0,B}$ while choosing $\phi_B = 0$ and $\theta_{0,C}$ while choosing $\phi_C = 0$.

[‡]for such cases, $\theta_0 > \theta_A$, which represents the structure of the whole polar cap region.

We thank Dr. Kejia Lee and other members in the pulsar group of Peking University for their helpful and enlightened discussions. Junwei Yu is grateful to Dr. Caiyan Li for her helpful assistance. The work is supported by NSFC (10973002,10935001), the National Basic Research Program of China (grant 2009CB824800).

REFERENCES

- Alcock, C. Farhi, E. & Olinto, A. 1986 ApJ, 310, 261
- Arons, J. & Scharlemann, E. T. 1979 ApJ, 231, 854
- Deshpande, A. A. & Rankin, J. M. 1999 ApJ, 524, 1008
- Drake, F. D. & Craft, H. D. 1968 Nature, 220, 231
- Fowlers, E. G. Lee, J. F. Ruderman, M. A. Sutherland, P. G. Hillebrandt, W. & Muller, E. 1977 ApJ, 215, 291
- Gil, J. Melikidze, G. & Zhang, B. 2006 ApJ, 650, 1048
- Goldreich, P. & Julian, W. H. 1969 ApJ, 157, 869
- Lai, D. 2001 Rev. Mod. Phys., 73, 629
- Medin, Z. & Lai, D. 2007 MNRAS, 382, 1833
- Melikidze, G. & Gil, J. 2009 The Eighth Pacific Rim Conference on Stellar Astrophysics ed B Soonthornthum, S. Komonjinda, Cheng, K. S. & Leung K. C. (San Francisco: Astronomical Society of the Pacific) 73, 131
- Qiao, G. J. Lee, K. J. Zhang, B. Xu, R. X. & Wang, H. G. 2004 ApJ, 616, 127
- Qiao, G. J. & Lin, W. 1998 A&A, 333, 172
- Ruderman, M. A. & Sutherland, P. G. 1975 ApJ, 196, 51
- Shukre, C. S. 1992 Magnetospheric Structure and Emission Mechanisms of Radio Pulsars, (IAU Colloq. 128) ed T H Hankins, J. M. Rankin, J. M. & Gil, J. A. (Pedagogical Univ. Press) p.412
- Usov, V. V. & Melrose, D. B. 1995 Aust. J. Phys., 48, 571
- Vivekanand, M. & Joshi, B. C. 1999 ApJ, 515, 398

- Xu, R. X. 2009 J. Phys. G: Nucl. Part. Phys., 36, 064010
- Xu, R. X. Cui, X. H. & Qiao, G. J. 2006 Chinese J. Astron. Astrophys., 2, 217
- Xu, R. X. & Qiao, G. J. 1998 Chin. Phys. Lett. 15, 934
- Xu, R. X. Qiao, G. J. & Zhang, B. 1999 ApJ, 522, L109
- Xu, R. X. Zhang, B. & Qiao, G. J. 2001 Astropart. Phys., 15, 101
- Zhang, B. Harding, A. K. & Muslimov, A. G. 2000 ApJ, 531, L135